BMC Oral Health

RESEARCH

Open Access

Combined use of deproteinized bovine bone mineral and α-tricalcium phosphate using gelatin carriers

Masako Fujioka-Kobayashi[1,2], Veronika Urbanova[1], Niklaus P. Lang[1,3], Hiroki Katagiri[4] and Nikola Saulacic[1*]

Abstract

Objective To study the effect on biomaterial degradation and bone formation of different ratios between α-tricalcium phosphate (α-TCP) and deproteinized bovine bone mineral (DBBM) using various gelatins as a carrier.

Materials and methods Thirty-six critical-sized calvarial bone defects were randomly treated in 18 animals. Four biomaterials with different compositional relations of DBBM to α-TCP and granules to carrier were investigated: (1) 40 ± 10% DBBM/40 ± 10% α-TCP with 20 ± 10% gelatin type 1 in ratio 4:1 (B1/G1), (2) 20 ± 10% DBBM/60 ± 10% α-TCP with 20 ± 10% gelatin type 1 in ratio 4:1 (B2/G1), (3) 20 ± 10% DBBM/60 ± 10% α-TCP with 15 ± 10%/5 ± 5% gelatin type 2/ glycerine (B2/G2) and 4), 10 ± 10% DBBM/60 ± 10% α-TCP with 20 ± 10%/10 ± 10% gelatin type 2/ glycerine (B3/G2). As a positive control 50 ± 10% DBBM/50 ± 10% α-TCP without gelatin (PC, B1/G0) and as a negative control (NC) empty defects were chosen. All defects were covered with a collagen membrane. The samples were harvested 4 weeks post-surgically and examined by micro-CT and histomorphometric analysis.

Results New bone formation was evident in all defects. The mineralized tissue volume was significantly higher in the four tested biomaterials than in the NC group, but lower compared to the PC group. Histomorphometry showed similar levels of bone formation in all groups, whereas only the PC group reached a significantly higher total augmentation area than that of the NC. The PC group showed significantly higher mineralized tissue density and residual material area compared to the B3/G2 group, and more residual DBBM than the four tested biomaterials.

Conclusions New bone formation was not significantly affected either by different DBBM:α-TCP compositional ratios nor the presence of various gelatin carriers.

Clinical relevance Similar levels of osteoconductivity indicates the presumptive use of combined products in alveolar ridge augmentation to support bone formation. Gelatin with or without glycerine may be considered for its use as a carrier to the biomaterials frequently applied in peri-implant surgery.

Keywords Deproteinized bovine bone mineral, α-tricalcium phosphate, Gelatin, Bone formation

*Correspondence:
Nikola Saulacic
Nikola.Saulacic@insel.ch
[1]Department of Cranio-Maxillofacial Surgery, Inselspital, Bern University Hospital, Bern, Switzerland
[2]Department of Oral and Maxillofacial Surgery, Shimane University Faculty of Medicine, Shimane, Japan
[3]Department of Periodontology, School of Dental Medicine, University of Bern, Bern, Switzerland
[4]Advanced Research Center, The Nippon Dental University School of Life Dentistry at Niigata, Niigata, Japan

Introduction

Applying biomaterials in combination with a barrier membrane is a highly predictable treatment [1]. However, the graft should possess appropriate features to allow three-dimensional stability with regards to the type of defect [2]. The characteristics of bone graft substitutes include biocompatibility and preferably osteoconductivity, as well as acting as a scaffold for new bone formation [3, 4]. Long-term success of guided bone regeneration (GBR) depends on the maintenance of the generated volume. Quality and quantity of bone formation largely depends on the granular size and porosity, as well as the chemical composition, the degree of hydrophilicity and capillarity of the substitute affecting the degradability [5]. The most commonly applied granular bone substitutes are the deproteinized bovine bone mineral (DBBM). This provides long-term volume stability [6–8]. DBBM is composed of mainly spongy bovine bone with a trabecular structure and internal voids free of organic components [9].The resorption speed of DBBM is relatively slow and is mediated by the osteoclastic activity [10]. Its resorption may result in a decrease of newly formed bone [11]. Thus, the DBBM granules were frequently applied in combination with autogenous bone [12]. In contrast, resorbable tricalcium phosphates (TCPs) are rapidly degraded and are replaced by newly formed bone. Hereby, the degradation rate of α-TCP was faster than that of β-TCP due to the differences in structure and solubility [13]. Fast degradation of both TCPs leads to an insufficient amount of newly formed mineralized bone [11], and hence, may limit the clinical efficacy. The degradation rate of α-TCP as well as the qualitative and quantitative new bone formation may be influenced by coverage of its surface with biomimetic hydroxyapatite and fine-tuned by the level of biomimetic hydroxyapatite (HA) coverage [14]. Actually, the higher HA content led to the lower rate of material degradation concomitant with the lower rate of new bone formation. In comparison to DBBM alone, a combination of DBBM with α-TCP in a compositional relation of 1:1 was osteocoductive and yielded minor resorption in a recent study [15]. Only α-TCP with DBBM showed increased mineral density when compared to DBBM alone [15]. Hence, it is possible that an increased percentage of the α-TCP to the DBBM would enhance bone formation as compared to the relation 1:1.

Numerous attempts have been made to improve the structure to optimize the osteoconductive capacity of the TCPs by introducing other components like hydrogels. Gelatin is a form of a hydrolyzed collagen, utilized for the bone regeneration due to its high biocompatibility, biodegradation, elasticity, and low antigenicity [16, 17]. Nevertheless, gelatin sponges cannot maintain dimensional stability [18]. Therefore, gelatin was cross-linked with glycerol phosphates [19] or combined with other polymers [20] to enhance its physico-chemical and biological characteristics. Formulation of demineralized bone matrix with gelatin and glycerol significantly enhanced the alkaline phosphatase activity when compared to the demineralized bone matrix alone [21]. Among others, methacrylate-based gelatin hydrogels were used to promote bone regeneration in situ [22]. Bioceramics including HA and TCP, bioglass, biomimetic scaffolds, inorganic ions and other organic components were added to the methacrylate-based gelatin to improve their osteogenic potential [22]. The scaffolding made of HA-gelatin [23] and aminosilane nanocomposite increased mineralization in vitro and bone formation in calvaria defects in vivo [24]. Gelatin sponges were successfully used to seal the extraction sockets filled with DBBM [25], but the application of the gelatin, with or without glycerine, as a carrier for biomaterials commonly used in peri-implant surgery has not been assessed as yet.

The aim of the present study was to assess the impact of different combinations of DBBM and α-TCP on bone formation. The effect of gelatin as a carrier of combined biomaterials on resorptive and osteoconductive potential was to be studied as well. The null-hypothesis was that of no difference in the osteoconductive potential of biomaterials composed of different DBBM to α-TCP ratios. The primary outcome was the amount of newly formed bone in critical-size rabbit calvaria bone defects.

Table 1 Weight% of each component (mineral and carrier) per group

Group	Biomaterials		Carrier
NC	-	-	-
PC (B1/G0)	50 ± 10%DBBM	50 ± 10%α-TCP	-
B1/G1	40 ± 10%DBBM	40 ± 10%α-TCP	20 ± 10% Gelatin
B2/G1	20 ± 10%DBBM	60 ± 10%α-TCP	20 ± 10% Gelatin
B2/G2	20 ± 10%DBBM	60 ± 10%α-TCP	15 ± 10% Gelatin / 5 ± 5% Glycerine
B3/G2	10 ± 10% DBBM	60 ± 10%α-TCP	20 ± 10% Gelatin / 10 ± 10% Glycerine

Materials & methods

Biomaterials

Biomaterials were used in a mixture of DBBM and α-TCP. Combined biomaterials were embedded in gelatin without glycerine (Type 1) or with glycerine (Type 2; Table 1; Figures S1 and S2). Biomaterials without gelatin served as a positive control (PC) and empty defects as a negative control (NC). All biomaterials were provided by Geistlich Pharma AG, Wolhusen, LU, Switzerland.

Animals

Eighteen New Zealand White female rabbits (approximately 16 weeks of age, weight 3.0–3.4 kg), were used. The animals were housed in the Central Animal Care

Facility at the University of Berne at a temperature of 19–21 °C, a humidity of 45%±10%, and a light/dark cycle of 12:12 h. The animals were fed with a standard diet and were provided water *ad libitum*. The study protocol considered the NC3Rs, UK guidelines, and was approved by the Committee for Animal Research, Canton of Bern, Switzerland (Nr: BE 89/17). In addition, the study complied with the ARRIVE 2.0 Guidelines.

Surgical procedures

The animals were premedicated and anesthesia was provided as previously described [14]. The rabbit skin was incised from the nasal bone to the mid-sagittal crest. The periosteum was elevated to expose the parietal bone. Two 10-mm diameter critical-size calvaria bone defects were prepared using a trephine under copious irrigation (Fig. 1A). Maximal care was taken to avoid injury to the *dura mater*. Intact parietal bone discs were harvested and used as a reference ($n = 8$). Six treatment modalities were allocated in 36 critical-size defects ($n = 6$ per group), randomized according to a systematic random protocol (www.randomization.com). Potential confounders were not specifically controlled. No sample size calculation was performed due to the exploratory nature of this study. From the auricular artery, 300 µL of blood were drawn to mix with each biomaterial and subsequently implanted into a defect (Fig. 1B) and another 300 µL were used to fill up the NC. All defects were covered with a collagen barrier membrane (BioGide, Geistlich Pharma AG, Wolhusen, Switzerland; Fig. 1C). The wounds were closed with interrupted sutures (4–0 Vicryl and 4–0 Monocryl Ethicon, Somerville, NJ, USA). Wound surfaces were further sealed with a spray film dressing (OPSITE SPRAY, Smith & Nephew, London, UK).

Following surgery, the animals were left to recover under infrared lights and application of oxygen. Postoperative analgesia consisted of meloxicam (Metacam®, Boehringer Ingelheim, Ingelheim, Germany) 0.5 mg/kg, *i.v.* administered after surgery and repeated once daily for 4 days. The animals were monitored at regular intervals and assessed for pain (composite pain scale and grimace scale). Buprenorphine (Temgesic®, Rechitt Benckiser, Wallisellen, Switzerland) was administered at 20 g/kg, *s.c.* every 8 h during the postoperative 3 days if indicated.

The animals were injected with Calcein red (0.6% Calcein/2% $NaHCO_3$, Sigma Aldrich, Chemie GmbH, Buchs, Switzerland) 10 mg/kg *i.p.* immediately after surgery and with Tetracycline hydrochloride (2%, Sigma Aldrich, Chemie GmbH, Buchs, Switzerland) 25 mg/kg *s.c.* three days before euthanasia.

After a healing period of 4 weeks, the animals were killed with an overdose of pentobarbital 120 mg/kg, *i.v.* (Streuli Pharma AG, Uznach, Switzerland) following the premedication (ketamine 65 mg/kg and xylazine 4 mg/kg, *s.c.*) in the neck area.

µCT analysis

The specimens were fixed in 10% neutral formalin for 7 days at room temperature. Subsequently, they were placed in 70% ethanol at 4 °C. They were trimmed and subjected to µCT scans using a desktop cone beam scanner (µCT 40, ScancoMedical AG, Brüttisellen, Switzerland) as previously described [14]. The X-ray source was set at 70 kV with 114 µA. An isotropic voxel size of 18 µm showed an image matrix of 2048 Å~ 2048 pixels. Following this, the µCT images were analyzed by using 3D structural analysis software (Amira, Thermo Fisher Scientific, Waltham, MA, USA). The primary volume of interest (VOI_1) was a 10-mm diameter cylinder.

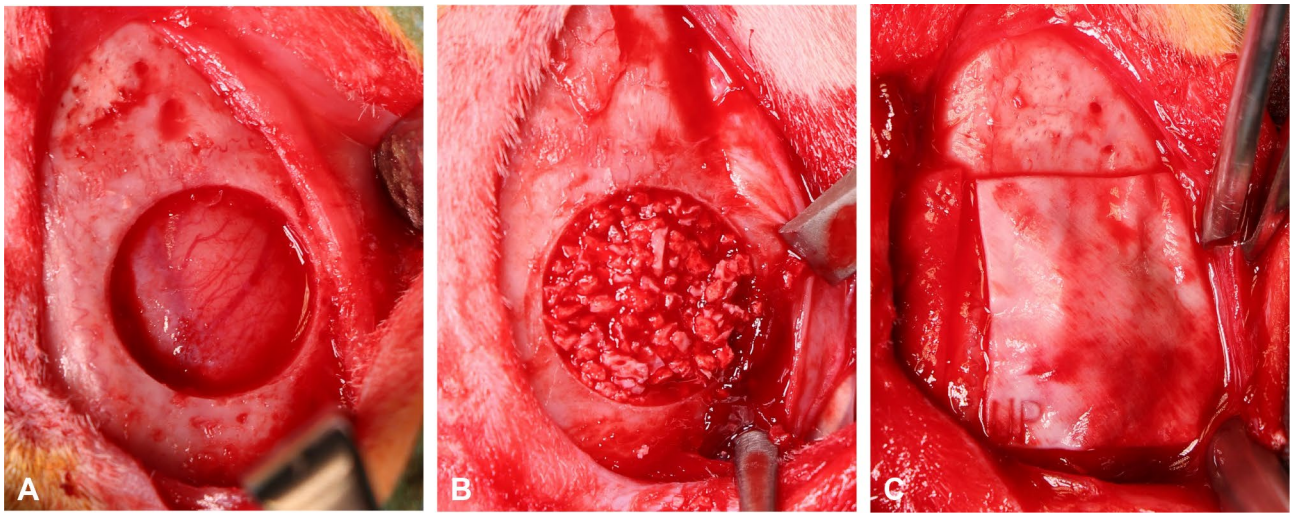

Fig. 1 Intra-operative images. Critical-size bone defects were created (**A**), and filled with the tested biomaterials (**B**). All sites were covered with a collagen membrane (**C**)

Mineralized tissue was selected on the greyscale images with the specific threshold set at 220 corresponding to the value of 530 mg HA/cm^3; voxels above this value were categorized as mineralized bone or background. Mineralized tissue volume MV (mm^3), MV/total tissue volume (MV/TV, %), mineral density (mgHA/cm^3) of the initial material (IMD), intact calvarial bone (IBD) and the defect sites at week 4 (BMD) were assessed. Moreover, horizontal defect closure (HDC, relative % to whole defect length; 10 mm) was calculated at the level of the most prominent bone ingrowth on the most-central sagittal sections (Figure S3 A, B).

Histological processing and histomorphometric analysis

After dehydration in ascending concentrations of ethanol, the specimens were embedded in methyl methacrylate without decalcification [26]. The tissue blocks were cut sagittal direction into approximately 800-µm thick blocks using a slow-speed diamond saw (VC- 50; LECO, St. Joseph, MI, USA). Following the mounting on acrylic glass slabs, the specimens were ground and polished to a final thickness of 200 µm (Knuth Rotor-3; Struers, Ballerup, Denmark). Then, they were stained with toluidine blue combined with fuchsin, and the images were photographed under a digital microscope (VHX-6000, Keyence, Japan). Quantitative histological analysis was performed on the central sections of each block applying a graphic software (Photoshop CC; Adobe, San Jose, CA, USA) and using the region of interest (ROI) that corresponded to the 10-mm initial defect area (Figure S1 C). Furthermore, a central 5-mm ROI in the defect sites (ROI-M), and the peripheral 2.5-mm ROI (ROI-L) were chosen. The parameters included the area densities (mm^2) of new bone (NBA), bone marrow (BMA), connective tissue (CTA), residual DBBM (RMA-DBBM), residual α-TCP (RMA-α-TCP), total residual material (RMA = RMA-DBBM + RMA-α-TCP), mineralized tissue (MTA = NBA + RMA) and total augmentation (TAA = NBA + BMA + CTA + RMA + MTA). Percentages of all area parameters were calculated relative to the TAA. Horizontal bone defect closure (HDC) was assessed in the sagittal plane on the third, mid-central sections of all samples. The osteoconductive capacity was evaluated in relation to the bone contact to granule surfaces in ROI-M and ROI-L in all specimens. The measurements were scored as 0 (without any bony contact), 0.5 (contact with one granule surface) or 1 (contact to one or more of granule surfaces; Figure S5). All measurements were performed by two blinded experienced examiners (M. F-K., I. G.).

Statistical analysis

The means and standard deviations (SD) for all parameters were calculated. Statistical analysis was performed by one-way analysis of variance (ANOVA) with a Tukey test by using a statistical program (GraphPad Prism X10 software: GraphPad Software, Inc., La Jolla, CA, USA). The level of significance was set at $\alpha = 0.05$.

Results

One animal had to be euthanized after surgery due to a neurological insult. No remaining animals ($n = 17$) showed any signs of local wound dehiscence, exposure of membranes, inflammation, or infection at the surgical sites. Three out of 34 defects were excluded from the analysis due to minor damage of the *dura mater* during surgery. The number of samples per group was $n = 5$ for the five groups with biomaterials and $n = 6$ for the NC group.

µCT analysis

All defects yielded new mineralized bone at the borders. However, this new bone could not be precisely distinguished from the residual bone substitute. Homogenously distributed mineralized structures were revealed throughout the defects for the PC (B1/G0) group comprising bone substitutes and newly formed bone (Fig. 2). The mineralized structures were less homogenous than in the PC (B1/G0) group in the four test groups showing enlarged non-mineralized spaces between the granules, especially for the B3/G2 group. All biomaterials showed greater MV and MV/TV in comparison to the NC (Fig. 3). Nevertheless, a significantly higher MV and MV/TV were observed only for the PC (B1/G0) group when compared to the four biomaterials tested.

The PC (B1/G0) and the B1/G1 showed significantly lower IMD values in comparison to the other three test groups ($p < 0.0001$, Figure S4). All biomaterials showed significantly higher IMD than the IBD. At the defect sites, all biomaterial groups showed higher MD than the NC group ($p < 0.0001$; Fig. 3). The HDC for B3/G2 was similar to that of the NC and the PC groups, whereas the other groups did not reach statistically significant difference (Fig. 3).

Histological analysis

In the peripheral area, all groups presented new mineralized bone and soft connective tissue in the center of the defects (Fig. 4). Light brownish and dark blue stained remnants of the gelatin Types 1 and 2 with surrounding cellular reactions were sporadically present in the middle part of the defects. Histomorphological analysis revealed that all groups presented similar values for NBA, BMA and HDC compared to the NC group in the ROI (Fig. 3), ROI_L and ROI_M (Fig. 5). Hence, none of the groups generated bone formation comparable to the initial bone. Only the PC (B1/G0) group showed significantly higher TAA than the NC group in the ROI. In the ROI-M, the TAA was significantly higher for granules with gelatin

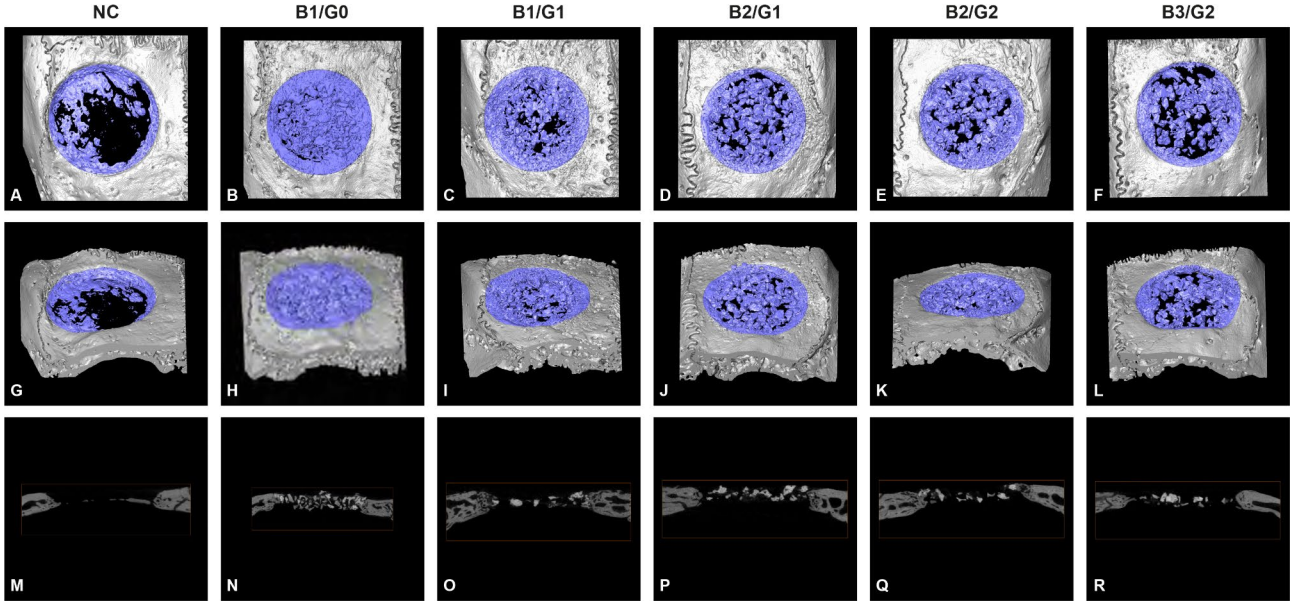

Fig. 2 Representative μCT images of the six groups at 4 weeks after surgery. Reconstructed 3D images from the top (**A**-**F**) and lateral view (**G**-**L**). The blue colour within the bone defects is showing mineralized tissue comprising newly formed bone and bone substitute materials. (**M**-**R**) Mid-central 2D sections of the corresponding sites

Type 1 than for the NC group, whereas granules with gelatin Type 2 showed lower values than the PC (B1/G0). All groups with biomaterials achieved higher MTA than the NC group except the B3/G2 group, being significantly lower in comparison to the PC (B1/G0) group (Fig. 3).

Both types of granules were detectable in all biomaterials (Fig. 4). In both types of biomaterials appositional bone formation was observed. The osteoconductive potential of all biomaterials tested was confirmed in magnified histological views in the peripheral areas of the defects (Fig. 6). The DBBM granules were well integrated into newly formed bone, without signs of degradation. The PC (B1/G0) and the B1/G1 showed significantly higher integration of the DBBM in the surrounding new bone as compared to other groups in the ROI-L, reaching statistical significance compared to the B3/G2 group (Fig. 5; $p = 0.006$). The α-TCP granules integrated in the bone demonstrated more irregular surfaces when compared to the granules integrated into the abundant fibrous connective tissue (Fig. 7). Irrespective of the presence of gelatin, bone tissue infiltrated the α-TCP granules in a mesh-like pattern. No differences in the osteoconduction potential between the groups were observed for the α-TCP granules in the ROI-L and ROI-M (Fig. 5).

All biomaterials with gelatin demonstrated lower RMA than the PC (B1/G0) group, reaching statistical significance for the B3/G2 in the ROI-L and ROI-M (Fig. 5). Within the soft tissue, DBBM granules sporadically underwent degradation. The RMA-DBBM was significantly lower in all groups with gelatin in comparison to the PC (B1/G0) group (Fig. 3). Furthermore, the B2/G2 and B3/G2 groups reached high statistical significance in comparison to the PC (B1/G0) group in the ROI-L and ROI-M (Fig. 5). Occasionally, both types of granules with gelatin Type 2 carriers were integrated within the same envelope of multinucleated giant cells (MNGC). In general, the MNGC appeared to be more frequently present around the α-TCP than around the DBBM granules, separated by fibrous tissue (Fig. 7). The RMA-α-TCP was similar between the groups (Fig. 3), while only B3/G2 demonstrated significantly lower RMA-α-TCP than the PC (B1/G0) in the ROI-L (Fig. 5).

Discussion

Analyzing the literature, yields that different degradation rates of biomaterials applied in GBR affected the amount of newly formed bone. It was, therefore, of interest to evaluate the composition of various biomaterials. The aim of the present study was to assess the effect of a combined use of DBBM with a rapidly degrading α-TCP on the biomaterial degradation and on new bone formation. The impact of gelatin as a carrier to promote ostoconductivity of a biomaterial has been demonstrated [21, 22]. Despite ongoing resorption, mineralized tissues areas have been maintained in situ in all groups tested in the present study. All biomaterials tested were proven to be osteoconductive. The absence of a statistically significant difference in NBA was not able to reject the null hypothesis. However, gelatin as a carrier to the biomaterials did not demonstrate a major benefit in the present model either.

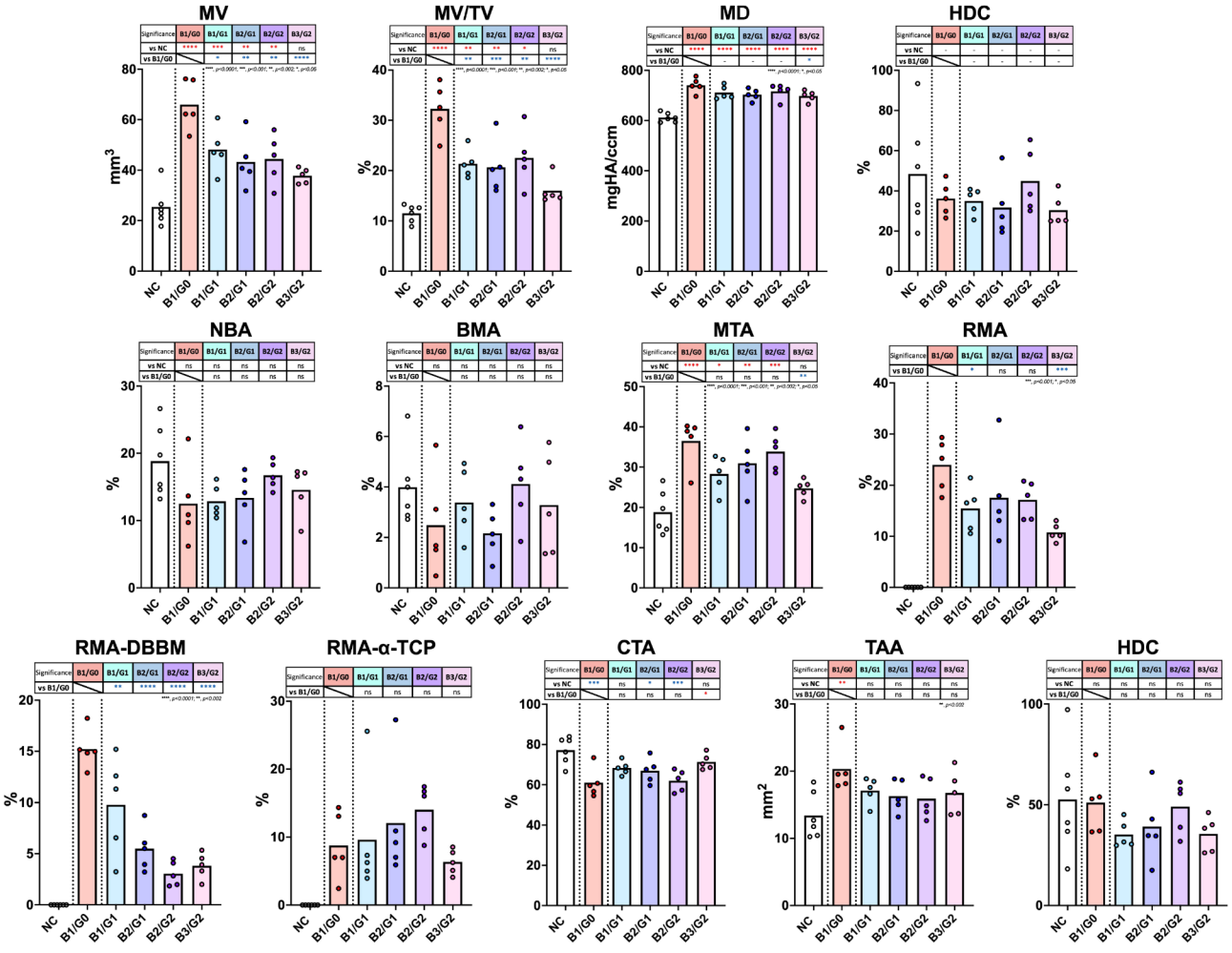

Fig. 3 µCT and histomorphometry parameters at 4 weeks post-surgery in the region-of-interest (ROI) of the whole defect. Quantification of µCT bone parameters showing mineralized tissue volume (MV), MV relative to the total tissue volume (MV/TV), mineral density (MD) and horizontal defect closure (HDC). Histomorphometric data of area parameters are analysed for new bone area (NBA), bone marrow area (BMA), mineralized tissue area (MTA), residual material area (RMA), residual α-TCP area (RMA-α-TCP), residual DBBM area (RMA-DBBM) and connective tissue area (CTA) relative to the total tissue area (TAA), and linear percentage of horizontal defect closure (HDC). Data are presented as bars with medians and individual data points. Statistical analysis was performed by one-way ANOVA followed by Tukey's multiple comparison test. *$p < 0.05$, **$p < 0.002$, ***$p < 0.001$, ****$p < 0.0001$

In the present study, rabbit calvaria critical-size defect model has been applied to evaluate osteoconductivity and new bone formation in combination with various bone substitutes and carriers. This model has been widely used in the study of bone formation. It is reliable, reproducible and representative for comparison [15]. New bone formation has been evaluated both by µCT and histomorphomeric analyzes. µCT revealed significantly increased MV and MV/TV for all biomaterials as compared to the NC, indicated the expected effect on scaffold forming in bone regeneration [14, 15]. Thus, significantly higher values for PC (B1/G0) compared to all test groups corroborated the findings of Santos et al. [27] showing lower BV/TV for HA mixed with gelatin and alginate in comparison to the DBBM. Less homogenously distributed mineralized structures were probably the result of remnant gelatin that occupied space between the granules. Although the IMD values for the PC (B1/G0) and B1/G1 were significantly lower than for the other three groups, this had no effect on the BMD at the defect sites. The BMD values in all groups significantly decreased when compared to the IMD, but was similar among the groups with biomaterials being significantly higher for all biomaterials than for the NC group.

The ratios between DBBM and α-TCP applied in the present study had been chosen arbitrarily, as the results of the 1:1 ratio were available [14]. Different ratios of DBBM and α-TCP yielded very similar bone formation volumes in the present study. Thus, the addition of α-TCP to DBBM in a ratio 4:1 did not jeopardize volume stability at an early healing stage. These findings are in line with the previously published data during early healing

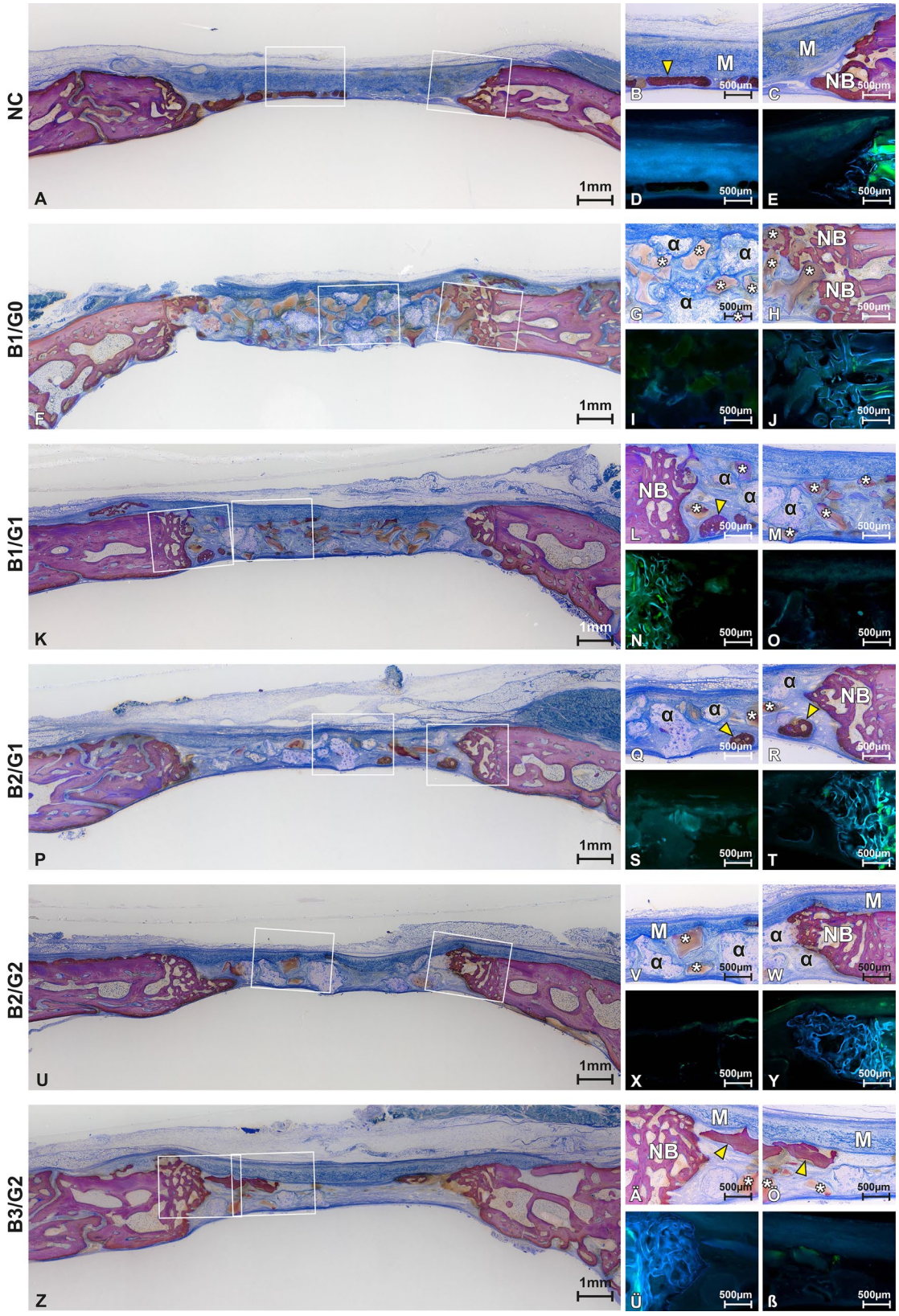

Fig. 4 Representative mid-sagittal histological sections. Boxed areas left are magnified right, with the corresponding fluorescence images. Ingrowth of the newly formed bone (NB) at the peripheral areas is observed in all groups. Signs of new bone formation within the defects (yellow arrowheads) are present at the periosteal or *dura mater* sides. Remnants of the membranes (M) are still detectable. In the central areas, the α-TCP (α) and DBBM (*) particles were frequently embedded in the abundant soft connective tissue. Toluidine blue with fuchsin staining

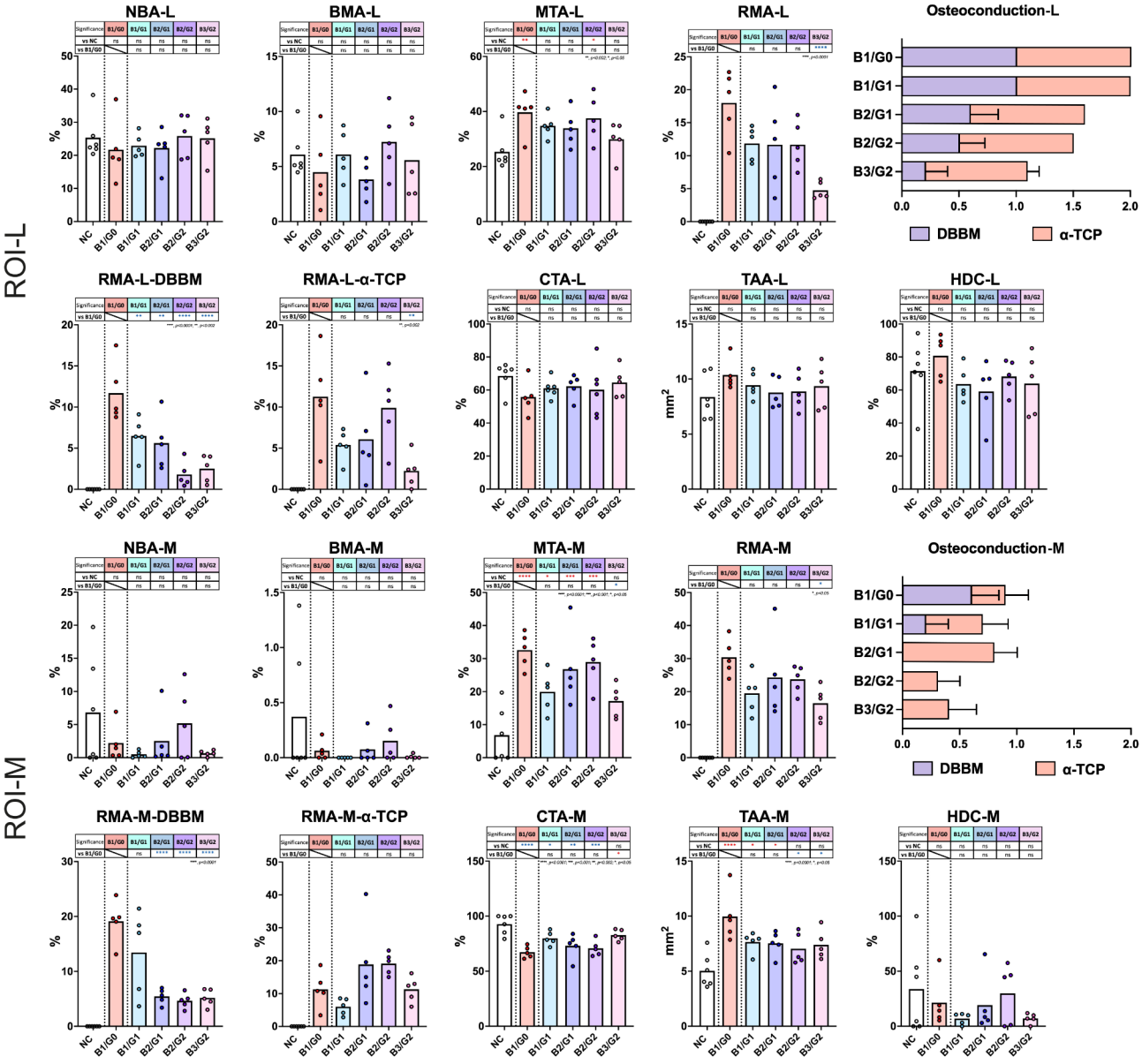

Fig. 5 Histomorphometry analysis at 4 weeks post-surgery in the lateral and middle region-of-interest (ROI-L and ROI-M, respectively). The parameters were analysed for new bone area (NBA), bone marrow area (BMA), mineralized tissue area (MTA), residual material area (RMA), residual α-TCP area (RMA-α-TCP), residual DBBM area (RMA-DBBM) and connective tissue area (CTA) relative to the total tissue area (TAA), and linear percentage of horizontal defect closure (HDC). Osteoconductive capacity was measured separately for α-TCP and DBBM particles. Data are presented as bars with medians and individual data points. Statistical analysis was performed by one-way ANOVA followed by Tukey's multiple comparison test. *$p < 0.05$, **$p < 0.002$, ***$p < 0.001$, ****$p < 0.0001$

on combined biomaterials using α-TCP [14] or β-TCP [28]. An increased ratio of carrier to biomaterial in the B3/G2 group was probably the reason for not reaching a statistically significant difference in MTA when compared to the NC. However, statistical significance was obtained for MTA and RMA percentages in comparison to the PC (B1/G0).

Histologically, limited new bone formation was observed for all biomaterials and for the non-augmented sites. Despite an expectation of DBBM to α-TCP in presence of the gelatin to provide more space for bone formation, the addition of gelatin had no impact on the osteoconductive capacity of α-TCP. Limited amounts of bone has been formed at the expense of α-TCP granules that were found to be in the process of resorption. The osteoconductive capacity of DBBM was, however, decreased by the presence of gelatin in the ROI-L. This corroborated the findings of Ramis et al. [29] showing lower osteoinductive potential for demineralized bone

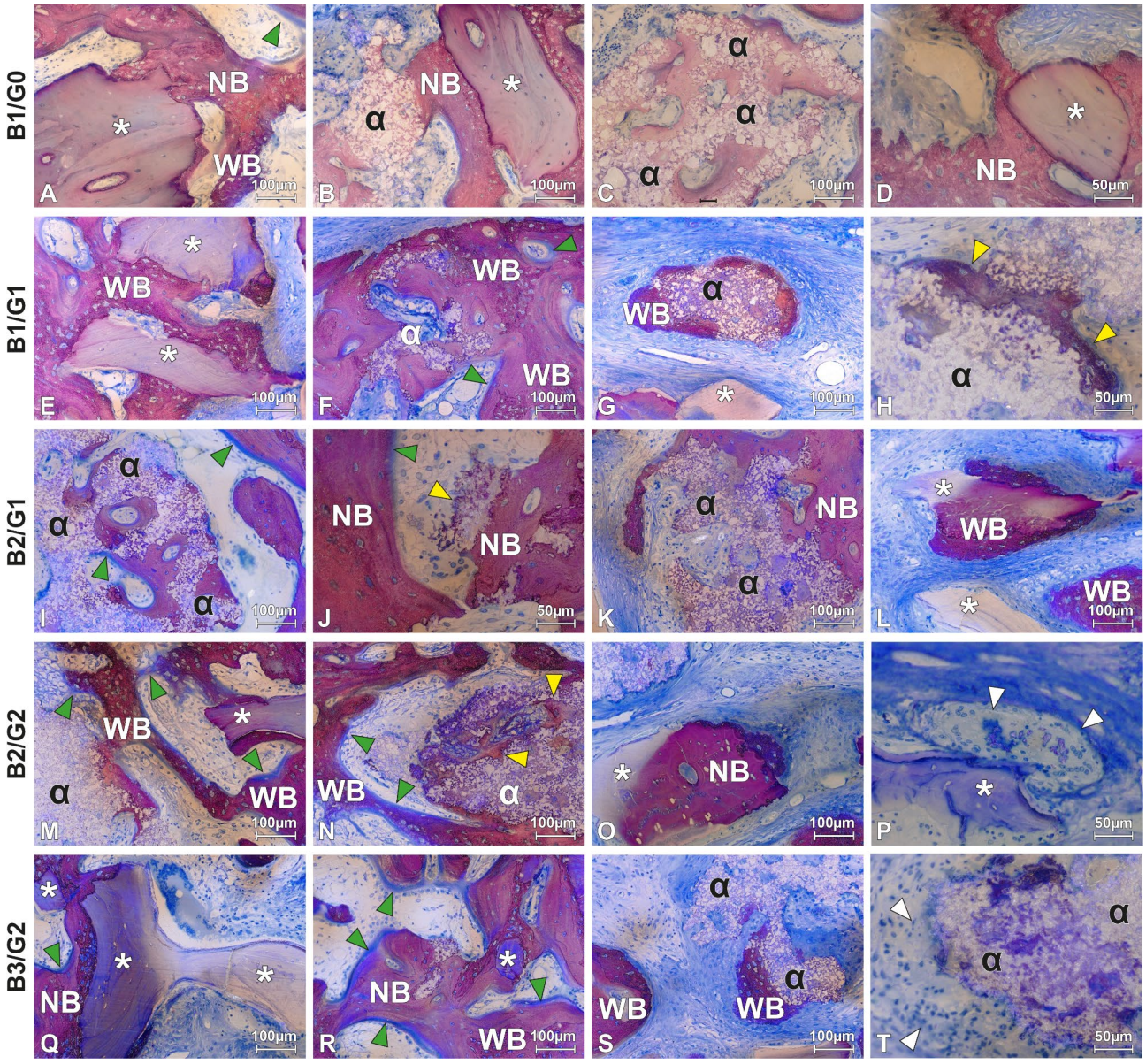

Fig. 6 Magnified views of the peripheral areas in groups with biomaterials. Mature new bone (NB) with signs of woven bone (WB) formation are observed in contact with the α-TCP (α) and DBBM particles (*). Osteoid (green arrowheads) is overlaying the surface of newly formed bone. Initial bone formation (yellow arrowheads) is seen at the periphery and within the α-TCP granules; this was not observed for the DBBM. Multinucleated giant cells (white arrowhead) are making contact with both types of the granules. Toluidine blue and fuchsin staining

matrix formulations with glycerol than with gelatin methacryloyl in the muscle of rats.

The results of the present study are in disagreement with the findings of Santos et al. [27]. This may be explained on the fact that different biomaterials had been used in the latter study. Significant differences in the osteoconductive potential demonstrated for B3/G2 compared to PC (B1/G0) and B1/G1 in the present study suggests that the ratio between the biomaterials and the carriers was more important than the type of carrier chosen.

Both types of biomaterials were surrounded by a numerous MNGCs in the ROI-M, but signs of DBBM osteoclastic resorption were rarely observed. As test groups differed in the initial amount of DBBM, this pattern seemed to be confirmed histologically in the defect sites at 4 weeks. Degradation of the α-TCP granules in the present study was frequently seen in the ROI-L. Nevertheless, no significant differences in the RMA-α-TCP between the groups was observed neither for ROI-L nor for ROI-M. The RMA-DBBM matched the compositional proportion of the corresponding biomaterial. As the DBBM is a slow osteoclastically resorbing bone substitute

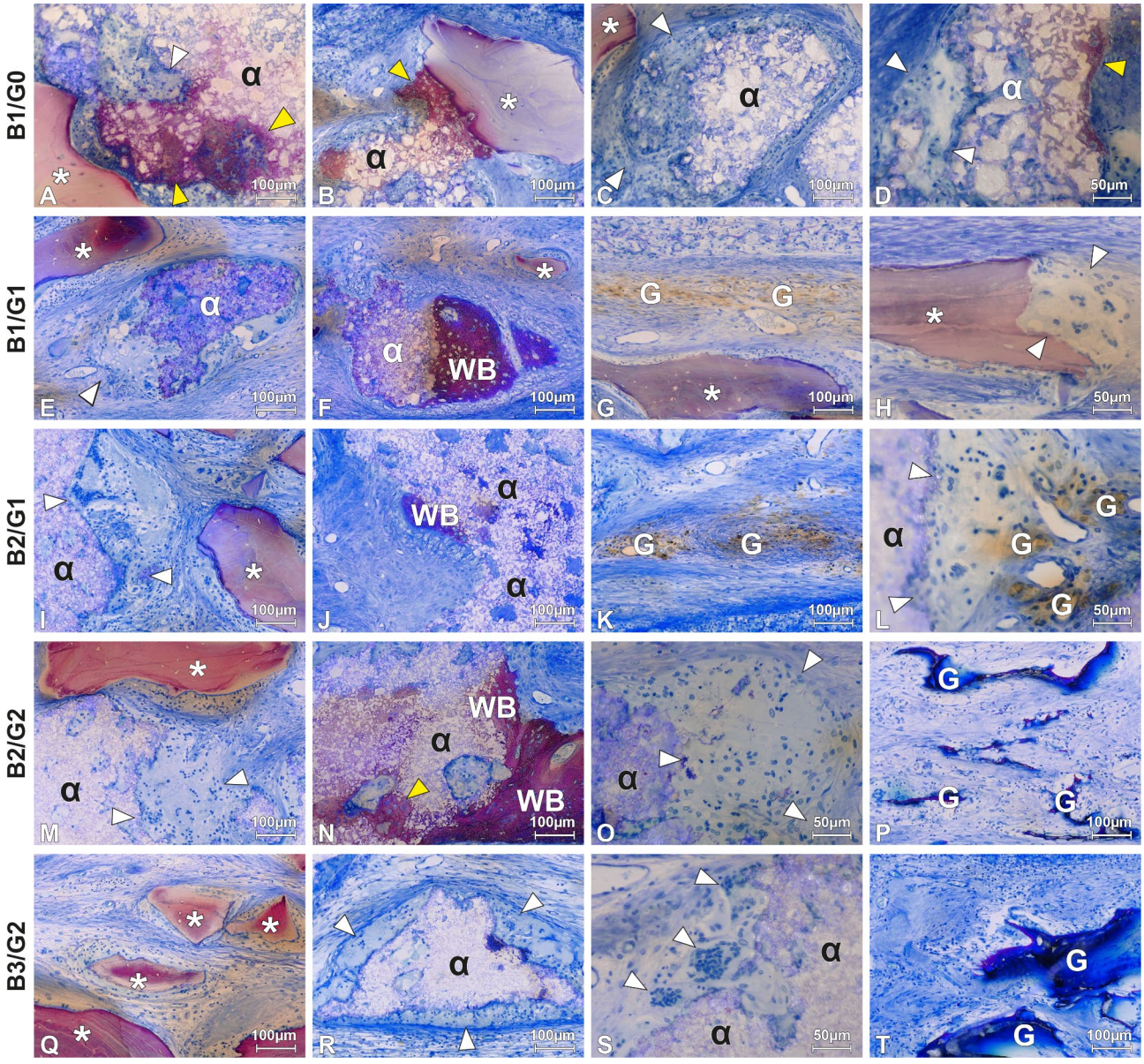

Fig. 7 Magnified views of the central areas in groups with biomaterials. Numerous multinucleated giant cells (white arrowheads) are seen surrounding both α-TCP (α) and DBBM particles (*), showing signs of biomaterial degradation. Initial mineralisation (yellow arrowheads) and woven bone (WB) formation are sporadically observed on the α-TCP particles. Remnants of the gelatin (G) were embedded in the soft connective tissue. Toluidine blue and fuchsin staining

[6, 7], this finding had to be expected. In future, quantitative analysis of the multinucleated giant cells will be considered to investigate a foreign body reaction to the biomaterials.

The results of the present study confirmed that gelatin with or without glycerine may be considered for its use in bone regeneration, showing favorable biocompatibility [21]. Since there were no previous data, the percentages of gelatin and glycerine were chosen deliberately. A single time-point of observation was, however, the limitation of the present study. The µCT and histological evaluations were seemingly not sensitive enough to yield differences in bone formation at an early stage. The detection of osteogenic differentiation and resorption markers may be more appropriate, showing different expression levels at 4-weeks of healing [28]. In a previous study [14], significantly more new bone volume and less residual material were observed at 3 months when compared to the 3 weeks healing period. Thus, it may be assumed that the combined biomaterials would have a greater impact on bone formation at later time of the remodeling phase (after the resorption of the α-TCP had been completed). Although significant progress has been made, the long-term response of gelatin to the microenvironment is to

be further investigated in terms of incorporation into the vascular network, in vivo degradation and bone regeneration at large [30].

Conclusions

The effect of different ratios between DBBM to α-TCP on *de novo* bone formation in the calvaria experimental model was minor. Limited resorption of the α-TCP was observed independently of the presence of gelatin, indicating similar levels of osteoconductivity for both combination products, α-TCP and DBBM. Further preclinical studies with longer-term healing periods are necessary to elucidate the potential benefits of bone substitute combinations.

Supplementary Information

The online version contains supplementary material available at https://doi.org/10.1186/s12903-025-05644-9.

Supplementary Material 1

Supplementary Material 2

Supplementary Material 3

Supplementary Material 4

Supplementary Material 5

Supplementary Material 6

Acknowledgements
The authors wish to thank the staff at Experimental Surgery Facility (ESF) and Central Animal Facilities (CAF), Department of BioMedical Research (DBMR), University of Bern, Switzerland, for their support of the animal surgeries and management. We also thank Ms. Inga Grigaitiene for her support of μCT image taking, histological preparation and histomorphometry.

Author contributions
Masako Fujioka-Kobayashi: study design, data acquisition, analysis and interpretation, statistics, manuscript drafting. Veronika Urbanova: data acquisition, analysis and interpretation, manuscript drafting. Niklaus P. Lang: study design, surgical planning, data interpretation and critically revised the manuscript. Hiroki Katagiri: conception, data analysis and interpretation, manuscript drafting. Nikola Saulacic: conception and study design, surgical planning and procedures, supervision and manuscript drafting. All authors gave their final approval and agree to be accountable for all aspects of the work.

Funding
This study was funded by Geistlich Pharma AG, Wolhusen, Switzerland.

Data availability
All data generated or analyzed during this study are included in this article and its supplementary information files. The data presented in this study are available on request from the corresponding author.

Declarations

Informed consent
Not applicable.

Institutional review board statement
The study was approved by the Committee for Animal Research, Canton of Berne, Switzerland (Nr: BE 89/17).

Competing interests
The authors declare no competing interests.

Received: 27 October 2024 / Accepted: 11 February 2025
Published online: 21 February 2025

References

1. Lang NP, Hammerle CH, Bragger U, Lehmann B, Nyman SR. Guided tissue regeneration in jawbone defects prior to implant placement. Clin Oral Implants Res. 1994;5:92–7.
2. Moy P, Palacci P. (2001) Minor bone augmentation procedures. Esthetic Implant Dentistry soft hard Tissue Manage, 137–58.
3. Titsinides S, Agrogiannis G, Karatzas T. Bone grafting materials in dentoalveolar reconstruction: a comprehensive review. Japanese Dent Sci Rev. 2019;55:26–32.
4. Yen CC, Tu YK, Chen TH, Lu HK. Comparison of treatment effects of guided tissue regeneration on infrabony lesions between animal and human studies: a systematic review and meta-analysis. J Periodontal Res. 2014;49:415–24.
5. Dutta S, Passi D, Singh P, Bhuibhar A. Ceramic and non-ceramic hydroxyapatite as a bone graft material: a brief review. Ir J Med Sci (1971-). 2015;184:101–6.
6. Zitzmann NU, Naef R, Schärer P. (1997) Resorbable versus nonresorbable membranes in combination with Bio-oss for guided bone regeneration. Int J Oral Maxillofacial Implants 12.
7. Baldini N, De Sanctis M, Ferrari M. Deproteinized bovine bone in periodontal and implant surgery. Dent Mater. 2011;27:61–70.
8. De Santis E, Lang NP, Ferreira S, Rangel Garcia I Jr., Caneva M, Botticelli D. Healing at implants installed concurrently to maxillary sinus floor elevation with Bio-oss(®) or autologous bone grafts. A histo-morphometric study in rabbits. Clin Oral Implants Res. 2017;28:503–11.
9. Figueiredo M, Henriques J, Martins G, Guerra F, Judas F, Figueiredo H. Physicochemical characterization of biomaterials commonly used in dentistry as bone substitutes—comparison with human bone. J Biomedical Mater Res Part B: Appl Biomaterials: Official J Soc Biomaterials Japanese Soc Biomaterials Australian Soc Biomaterials Korean Soc Biomaterials. 2010;92:409–19.
10. Jensen SS, Gruber R, Buser D, Bosshardt DD. Osteoclast-like cells on deproteinized bovine bone mineral and biphasic calcium phosphate: light and transmission electron microscopical observations. Clin Oral Implants Res. 2015;26:859–64.
11. Broggini N, Bosshardt DD, Jensen SS, Bornstein MM, Wang CC, Buser D. Bone healing around nanocrystalline hydroxyapatite, deproteinized bovine bone mineral, biphasic calcium phosphate, and autogenous bone in mandibular bone defects. J Biomed Mater Res B. 2015;103:1478–87.
12. Buser D, Chappuis V, Kuchler U, Bornstein MM, Wittneben JG, Buser R, Cavusoglu Y, Belser UC. Long-term stability of early implant placement with contour augmentation. J Dent Res. 2013;92:S176–82.
13. Carrodeguas RG, De Aza S. Alpha-tricalcium phosphate: synthesis, properties and biomedical applications. Acta Biomater. 2011;7:3536–46.
14. Saulacic N, Fujioka-Kobayashi M, Kimura Y, Bracher AI, Zihlmann C, Lang NP. The effect of synthetic bone graft substitutes on bone formation in rabbit calvarial defects. J Mater Sci: Mater Med. 2021;32:14.
15. Fujioka-Kobayashi M, Katagiri H, Lang NP, Imber JC, Schaller B, Saulacic N. (2022) Addition of synthetic biomaterials to deproteinized bovine bone Mineral (DBBM) for bone Augmentation-A preclinical in vivo study. Int J Mol Sci 23.
16. Kuttappan S, Mathew D, Nair MB. Biomimetic composite scaffolds containing bioceramics and collagen/gelatin for bone tissue engineering - A mini review. Int J Biol Macromol. 2016;93:1390–401.
17. Ranganathan S, Balagangadharan K, Selvamurugan N. Chitosan and gelatin-based electrospun fibers for bone tissue engineering. Int J Biol Macromol. 2019;133:354–64.
18. Ying Y, Li B, Liu C, Xiong Z, Bai W, Li J, Ma P. A biodegradable gelatin-based nanostructured sponge with space maintenance to enhance long-term osteogenesis in maxillary sinus augmentation. J Biomater Appl. 2021;35:681–95.
19. Cetin D, Kahraman AS, Gumusderelioglu M. Novel scaffolds based on poly(2-hydroxyethyl methacrylate) superporous hydrogels for bone tissue engineering. J Biomater Sci Polym Ed. 2011;22:1157–78.

20. Singh YP, Dasgupta S. Gelatin-based electrospun and lyophilized scaffolds with nano scale feature for bone tissue engineering application: review. J Biomater Sci Polym Ed. 2022;33:1704–58.
21. Zhao Y, Han L, Yan J, Li Z, Wang F, Xia Y, Hou S, Zhong H, Zhang F, Gu N. (2017) Irradiation Sterilized Gelatin-Water-Glycerol Ternary Gel as an Injectable Carrier for Bone Tissue Engineering. *Advanced healthcare materials* 6.
22. Zhou B, Jiang X, Zhou X, Tan W, Luo H, Lei S, Yang Y. GelMA-based bioactive hydrogel scaffolds with multiple bone defect repair functions: therapeutic strategies and recent advances. Biomater Res. 2023;27:86.
23. Chang MC, Ko CC, Douglas WH. Preparation of hydroxyapatite-gelatin nanocomposite. Biomaterials. 2003;24:2853–62.
24. Chiu CK, Ferreira J, Luo TJ, Geng H, Lin FC, Ko CC. Direct scaffolding of biomimetic hydroxyapatite-gelatin nanocomposites using aminosilane cross-linker for bone regeneration. J Mater Sci: Mater Med. 2012;23:2115–26.
25. Debel M, Toma S, Vandenberghe B, Brecx MC, Lasserre JF. Alveolar ridge dimensional changes after two socket sealing techniques. A pilot randomized clinical trial. Clin Oral Invest. 2021;25:1235–43.
26. Schenk R, Olah A, Hermann W. (1984) *Preparation of calcified tissue for light microscopy. In: Dickson, G.R., ed. Methods of calcified tissue preparation.*
27. Santos ACD, Aroni MAT, Pigossi SC, Lopes MES, Cerri PS, Miguel FB, Santos SRA, Cirelli JA, Rosa FP. A new hydroxyapatite-alginate-gelatin biocomposite favor bone regeneration in a critical-sized calvarial defect model. Braz Dent J. 2024;35:e245461.
28. Kunert-Keil C, Scholz F, Gedrange T, Gredes T. Comparative study of biphasic calcium phosphate with beta-tricalcium phosphate in rat cranial defects—A molecular-biological and histological study. Annals Anatomy-Anatomischer Anzeiger. 2015;199:79–84.
29. Ramis JM, Blasco-Ferrer M, Calvo J, Villa O, Cladera MM, Corbillo C, Gaya A, Monjo M. Improved physical and osteoinductive properties of demineralized bone matrix by gelatin methacryloyl formulation. J Tissue Eng Regen Med. 2020;14:475–85.
30. Zhu Y, Yu X, Liu H, Li J, Gholipourmalekabadi M, Lin K, Yuan C, Wang P. Strategies of functionalized GelMA-based bioinks for bone regeneration: recent advances and future perspectives. Bioact Mater. 2024;38:346–73.

Publisher's note